Swept Centerband Decoupling as a Technique in Nuclear Magnetic Double Resonance Spectroscopy

Thesis by

ANTON EMIL PIETSCH

In Partial Fulfillment of the Requirements

For the Degree of

Master of Science

California Institute of Technology

Pasadena, California

1976

TO MY PARENTS

ACKNOWLEDGEMENT:

I wish to express my gratitude to my research advisor, Professor John D. Roberts, for having given me the opportunity to develop my own ideas. I also thank Mr. I. Moskovitz and Mr. T. Dunn of the Chemistry Department Electronics Shop for their help and for some of their ideas that became part of the DFS-60 nmr spectrometer, and Dr. William H. Bearden for his assistance in interpreting some of my results.

ABSTRACT

A technique of doubly modulated radiofrequency irradiation to achieve nuclear magnetic spin-spin decoupling was developed. The effectiveness of this technique, called Swept Centerband Modulation, was investigated by comparison study with other well known techniques. It was found that swept centerband modulation produced an averaging of single coherent frequency decoupling over an adjustible bandwidth. The conclusion drawn from the study was that this technique is not effective for wide band decoupling but very effective for medium to narrow band selective decoupling experiments.

I. Introduction

The first modulated nuclear magnetic double resonance technique was introduced by Anderson and Nelson[1] in 1963. It involved audio sine wave modulation of the decoupling radiofrequency to eliminate residual couplings remaining in single frequency decoupling. The method was later formalized by Anderson and Freeman[2], and modulation methods have been developed to achieve more efficient decoupling over wider bands.

Wide band modulation was formalized by Ernst[3] in 1966, and in the same paper proposed the use of audio white noise as a practical method of modulation to generate a wide band decoupling spectrum. This was quickly replaced by pseudorandom binary noise modulation which gave more efficient decoupling for the amount of RF power available.[3]

The introduction of Fourier transform techniques about the same time as noise decoupling generated a great deal of interest in natural abundance spectroscopy of many nuclei.[4] The field has continued to expand, and spectroscopic techniques for both wide band and narrow band heteronuclear decoupling have become routine. More recent developements in the areas of large sample probes and high field superconducting solenoids have created new problems in wide band decoupling.[5] The wider band of decoupling frequencies needed in higher field spectrometers require additional RF power to remain effective, as does a larger sample volume to be irradiated. The required additional RF power has created excessive sample heating and hence has generated renewed interest in effective wide band methods.[6]

II. Basis for Development of Swept Centerband Modulation

A. Theoretical Treatment

Anderson and Freeman[2] have provided formal expressions for residual splitting in weakly coupled systems for the single coherent frequency and audio sine wave modulated decoupling schemes. Their work formed a basis on which expressions for coherent square wave[6] modulation and frequency independent power spectrum (wide band noise) modulation[3]. Decoupling efficiency is quantized in terms of J_r, the residual splitting or b_r, the line broadening in the highly decoupled case.

1. Single Coherent Frequency

The residual splitting for a single coherent frequency is[2]

$$2\pi J_r = \lfloor (\Delta\omega - \pi J)^2 + (\gamma^S H_2)^2 \rfloor^{1/2} - \lfloor (\Delta\omega + \pi J)^2 + (\gamma^S H_2)^2 \rfloor^{1/2} \qquad (1)$$

For a sufficiently large driving rf field $| H_2 | \gg | \Delta\omega / \gamma^S |$, this reduces to

$$J_r = J \Delta\omega / \gamma^S H_2 \qquad (2)$$

where $\Delta\omega = \omega^S - \omega_2$, the difference between the Larmor frequency of spin S, ω^S, and the irradiation frequency, ω_2 ; γ^S is the gyromagnetic ratio of spin S ; J is the splitting with no decoupling applied ; and H_2 is the field generated in the decoupling coil. It can be seen from these equations that single frequency decoupling has a large dependence on the difference frequency and is therefore effective only for a narrow band of frequencies at reasonable rf power levels.

2. Coherent Single Audio Frequency Modulation

Residual splitting for a centerband of field strength H_c and two equidistant sidebands of field strength H_s was expressed by Anderson and Freeman as[2]

$$2\pi J_r = \left\{ \left[(\Delta\omega + \pi J)^2 + (\gamma^S H_c)^2 \right]^{1/2} - \omega_m \right\}^2 + (\gamma^S H_s)^2 \Big]^{1/2} - \left\{ \left[(\Delta\omega + \pi J)^2 + (\gamma^S H_c)^2 \right]^{1/2} - \omega_m \right\}^2 + (\gamma^S H_s)^2 \Big]^{1/2} \quad (3)$$

where

ω_m is the audio modulation frequency which generates the sidebands by either frequency or amplitude modulation of the centerband. If sufficient rf power is used such that

$$| H_c |, | H_s | \gg | \Delta\omega / \gamma^S |, | \Delta\omega_o / \gamma^S |, 2\pi | J / \gamma^S |$$

then this equation can be reduced to

$$J_r = J (\Delta\omega^2 - \Delta\omega_o^2) \Delta\omega / [2 (\gamma^S H_c)^2 (\gamma^S H_s)^2] \quad (4)$$

where $\Delta\omega_o = [\omega_m^2 - (\gamma^S H_c)^2]^{1/2}$

The residual splitting is 0 for $\Delta\omega = 0, \pm \Delta\omega_o$ and has local maxima situated in between the centerband and the two sidebands. This makes the effective decoupling a function of the centerband setting even when the Larmor frequency lies within the modulation range.

3. Coherent Square Wave Modulation

Grutzner and Santini[7] have recently developed a more efficient modulation scheme for some wide band applications based on the Anderson and Freeman formalism for audio sideband modulation. The scheme they utilized phase modulates the centerband with

a 50% duty cycle square wave, which generates very large first sidebands and a very small centerband. The expression for the residual coupling is equation (3), setting $H_c=0$, and using the harmonic sidebands closest to ω_S as the largest contribution to decoupling, giving

$$2\pi J_r = \{ [B(+) - 2(n-m) \omega_m]^2 + [2 \gamma^S H_2 / (2m+1) \pi]^2 \}^{1/2}$$

$$- \{ [B(-) - 2(n-m) \omega_m]^2 + [2 \gamma^S H_2 / (2m+1) \pi]^2 \}^{1/2} \qquad (5)$$

where $B(\pm) = \{ [\Delta\omega \pm \pi J - (2n+1) \omega_m]^2 + [2 \gamma^S H_2 / (2n+1) \pi]^2 \}^{1/2}$

and m is an integer greater than n. This gives a residual coupling of zero when $\omega_S = (2n+1) \omega_m$, $n = 0, 1, 2, \ldots$, with the maximum effective n determined by whether H_2 for the 2n+1 th sideband is greater than approximately twice the magnitude of $2\pi J / \gamma^S$. This modulation method has local maxima residual splittings larger than those of optimized single sine wave modulation for the same modulation frequency, but covers a much wider band due to the higher sidebands generated.

4. Incoherent Wide Band Modulation

Ernst[3] determined an expression for residual coupling over a wide band of Larmor frequencies if several assumptions are made about the modulation technique. First, the bandwidth of the modulation must be larger than the band of Larmor frequencies so that band edge effects can be ignored. The second assumption is that the power density is constant and continuous over the entire modulation bandwidth. The expression for the line broadening, b_r, is given as

$$2\,\gamma^S H_2 = \left[(2/\pi)(J/b_r)(2\pi J/2\Delta\omega_t) \right]^{1/2} 2\Delta\omega_t \qquad (6)$$

which rearranges to

$$b_r = \Delta\omega_t \, (2J/\gamma^S H_2)^2, \qquad (7)$$

where $2\Delta\omega_t$ is the bandwidth of the modulation. This equation describes the effectiveness of the "ideal" wide band decoupling spectrum. By ideal, I mean a decoupling scheme that produces a rectangular power spectrum with no power dissipated outside of the desired band width.

5. Swept Centerband Modulation

The double modulation generated by single frequency with a sawtooth triangle wave does not lend itself to a simple analysis. The expression for the signal generated is

$$f(t) = A_o \sin\left\{ \left[\omega_o + \omega_d \left(2/\pi \sum_{n=1}^{\infty} \{(-1)^{n+1}/n\} \sin(n\omega_m t) \right) \right] t \right\} \qquad (8)$$

where ω_o is the centerband frequency, ω_d is the deviation from the centerband which determines the scan width, and ω_m is the frequency at which the scan is modulated. If $\omega_m = 0$, then this equation reduces to an expression for a single frequency at ω_o. For the experiments performed with swept centerband modulation, the constraint of $\omega_o \gg \omega_d \gg \omega_m$ was maintained, and the effects of this modulation may be approximated by the residual splitting equation for a single coherent frequency averaged over a specified bandwidth.

This is accomplished by integrating the residual splitting over the scan width ω_d and normalizing for the power density as in equation (9).

$$J_{r(ave)} = \frac{\int_{\omega_S-(\omega_o-\omega_d/2)}^{\omega_S-(\omega_o+\omega d/2)} \left[(\Delta\omega - \pi J)^2 + (\gamma^S H_2)^2 \right]^{1/2} - \left[(\Delta\omega + \pi J)^2 + (\gamma^S H_2)^2 \right]^{1/2} d\Delta\omega}{2\pi \int_{\omega_S-(\omega_o-\omega_d/2)}^{\omega_S-(\omega_o+\omega_d/2)} d\Delta\omega} \qquad (9)$$

which becomes (see appendix A)

$$J_{r(ave)} = (1/4\pi\omega_d) \left\{ (\Delta\omega - \pi J) \left[(\Delta\omega - \pi J)^2 + (\gamma^S H_2)^2 \right]^{1/2} \right.$$

$$+ (\gamma^S H_2)^2 \operatorname{arcsinh} \left[(\Delta\omega - \pi J) / (\gamma^S H_2) \right]$$

$$- (\Delta\omega + \pi J) \left[(\Delta\omega + \pi J)^2 + (\gamma^S H_2)^2 \right]^{1/2}$$

$$\left. - (\gamma^S H_2)^2 \operatorname{arcsinh} \left[(\Delta\omega + \pi J) / (\gamma^S H_2) \right] \right\} \Bigg|_{\omega_S-(\omega_o-\omega_d/2)}^{\omega_S-(\omega_o+\omega_d/2)} \qquad (10)$$

The foregoing expressions are not entirely rigorous because second order modulation effects have been eliminated. In addition, the assumption is made that many scans are made during data collection on the observe channel, which is valid for FT experiments where many transients are collected.

For a sufficiently large rf driving field $| \gamma^S H_2 | \gg | \Delta\omega |$, Equation (10) reduces to

$$J_{r(ave)} = (1/(4\pi\omega_d)) \{ (\Delta\omega - \pi J) \lfloor (\Delta\omega - \pi J)^2 + (\gamma^S H_2)^2 \rfloor^{1/2} - (\Delta\omega + \pi J) \lfloor (\Delta\omega + \pi J)^2 + (\gamma^S H_2)^2 \rfloor^{1/2} \Big|_{\omega_S-(\omega_o-\omega_d/2)}^{\omega_S-(\omega_o+\omega_d/2)} \quad (11)$$

which may be qualitatively described as a response similar to that of single coherent frequency. When the Larmor frequency falls outside the range of the scanning frequency, the residual coupling increases as if it were irradiated by a single stationary frequency. When the Larmor frequency is within the range of the scanning frequency, the response is nearly the same for any center frequency and is represented as a broad hump centered at $\omega_S = \omega_o$.

B. Determination of Decoupler Efficiency via a Spectrum Analyzer

Grutzner and Santini describe the use of a spectrum analyzer in their determination of the effectiveness of coherent square wave modulation.[7] I followed their guidelines in performing several comparison tests of various decoupling schemes. All tests were accomplished using a Tektronics 7603 oscilloscope mainframe with a 7L12 spectrum analyzer plug-in.

1. Test of the Spectrum Analyzer Resolution

Fig. 1 shows the test set-up for determining the response of the spectrum analyzer, which was utilized because it provides a very close measure of the actual signals irradiated to the sample in a NMR experiment. The frequency synthesizer was set at a constant frequency of 20.005000 MHz and left unmodulated by the mixer. The maximum resolution setting available on the analyzer plug-in was 300 Hz, and the maximum spectrum expansion was 500 Hz / DIV. The 300-Hz resolution limit corresponds to a signal analyzed with the analyzer demodulation oscillator free running, but some signals could be phase-locked and higher resolution achieved. The response of the spectrum analyzer to a single sharp frequency that was not phase-locked is shown in Fig. 2. The vertical response is a logarithmic plot of total power at the demodulated frequency (10 dB / DIV). A sweep rate of ~1 DIV / Second was used to achieve a high resolution over the 5 KHz band swept on the horizontal axis. These settings were used for all but one (noted) of the photographs, and the response in Figure 2 is therefore a good reference by which to gauge the spectrum analyzer.

2. Noise Modulated Spectrum

The most conventional electronic method for accomplishing wide band decoupling is binary noise modulation. Figure 3 represents the experimental set-up for observing a noise modulated spectrum, using a Hewlett-Packard 3722A noise generator as the source of binary noise. The frequency synthesizer was set at 20,005,000 Hz and the noise generator placed in its "INFINITE" cycle mode. The INFINITE setting produces a random, non-repetitive sequence of pulse widths. Figures 4a to 4d demonstrate the response of the spectrum analyzer to several clock periods commonly used with Caltech's DFS-60 NMR spectrometer(see Instrumentation section). Clock periods of 1ms, 3.33ms, 10ms, and 33.3ms correspond to primary bandwidths of 2000 Hz, 600 Hz, 200 Hz, and 60 Hz,respectively. It can most easily be seen from Figure 4d that binary noise modulation dissipates a large amount of power outside the primary bandwidth at odd harmonics of the clock frequency.

3. Coherent Square Wave Modulation

Square wave phase modulation into a balanced mixer as described by Grutzner and Santini[7] produces a series of sidebands spaced at $(2n+1) \omega_m$ intervals (odd harmonics of the modulation frequency) about the centerband with intensities corresponding to $(2n+1)^{-2}$ for $n = 0, 1, 2, \ldots$ The test apparatus for square wave modulation is as shown in Figure 5. Figures 6a to 6c demonstrate the large amount of power dissipated at the higher harmonics not useful for decoupling.

4. Swept Square Wave Modulation

Swept square wave modulation is utilized in Caltech's Bruker WH-180

NMR Spectrometer. A test set-up to simulate WH-180 conditions for this modulation scheme is represented in Fig. 7. The square wave generator is driven by a triangle wave generator such that the modulation frequency is monotonically swept over a specified range. This double-modulation technique can be graphically represented by a series of odd harmonics of the various frequencies within the range swept by the triangle wave. Fig. 8a-d demonstrates the power spectra generated by swept square waves for various modulation ranges. Once again, not all of the power is found within a useful decoupling region, and a dip in the power spectra exists at the centerband.

5. Swept Centerband Modulation

This technique has its name derived from the fact that modulation is accomplished through the use of the search oscillator found within the frequency synthesizer, where the centerband is normally determined. The search oscillator is a voltage-controlled oscillator whose frequency varies linearly over a range with variations in the control voltage. It may be inserted at any decade digit between 1Hz and 1MHz to give the desired range of control and stability in a direct synthesis frequency generator. The apparatus in Fig. 9 shows the frequency synthesizer search oscillator driven by a device constructed to generate the desired monotonically swept centerband. The schematic for this device is shown in Fig. 10. It produces a sawtooth triangle wave superimposed on a precise DC voltage. The average DC voltage determines the center of the frequency range, the amplitude of the sawtooth determines the range over which the frequency is scanned, and the frequency of the sawtooth determines the rate at which the rf is scanned.

The results shown in Figures 11a to 11d indicate that swept centerband modulation produces a nearly flat power spectrum over the desired bandwidth with little power dissipated outside of that range. On the basis of these positive results, further research was conducted to fully parameterize the effects of swept centerband decoupling.

III. Experimental

A. Instrumentation

All ^{13}C spectra shown were collected on Caltech's DFS-60 spectrometer operating at a proton resonance of 60MHz. The decoupler synthesizer, observe synthesizer, heteronuclear internal ^{2}H lock unit, and computer timing circuitry are all locked together on a 1MHz TCXO in the decoupler synthesizer driver. Observation was done at 15.09MHz for ^{13}C using a single coil double tuned (^{13}C, ^{2}H) 10 mm probe. The decoupling frequency generation scheme at 60.00MHz (^{1}H) is shown in Fig. 12. For noise decoupling the noise generator is in the RUN mode set for INFINITE cycle and the search oscillator in the frequency synthesizer is not used. Single frequency decoupling is accomplished by placing the noise generator in the RESET mode (constant DC current output) and digitally selecting the desired frequency on the synthesizer. Swept centerband decoupling occurs when a search digit is selected on the synthesizer with the noise generator set in RESET mode to bias the mixer. This method insures that the decoupling power will be equal for the same attenuator setting in all three modes of operation. The centerband in swept decoupling mode is monitored by using a Hewlett-Packard 5245L frequency counter with its time base driven by the 1MHz system frequency. A maximum decoupler power of 11.8 W delivered at the probe produces an effective field ($\gamma^{S} H_2 / 2\pi$) of $\cong$ 3000 Hz as determined in appendix B.

The proton spectrum was collected on a standard Varian T-60.

B. Samples

1. Dioxane

A 80% Dioxane, 20% D_2O sample prepared from reagent grade chemicals has been used with the DFS-60 as a calibration standard, and was utilized as a simple AX system for determining the response to offset variations for swept centerband decoupling. FT data was collected for a 1200Hz bandwidth with a 2 second acquisition time and a 4 second pulse delay. A 90 degree pulse width of 28 microseconds was utilized on all spectra collected.

2. p-Chloronitrobenzene in Ethyl Acetate

The sample was prepared from reagent grade chemicals without further purification by stirring an excess amount of p-chloronitrobenzene in ethyl acetate to obtain a saturated solution. 1 ml of Silanor-C was added for locking purposes to ~ 3 ml of saturated solution in the sample tube and a vortex plug inserted. Spectra were collected with a 12 microsecond pulse width (~ 40 degree) over a bandwidth of 5KHz. FT data using 8K of memory was obtained with an acquisition time of .8 seconds and a pulse delay of 3.2 seconds.

C. Results

Swept centerband decoupling is closely analogous to the rapid adiabatic passage technique for CW data collection. If the driving frequency is repetitively swept very rapidly such that the repetition frequency is greater than the bandwidth of the receiver, then the demodulated output becomes a measure of the average signal intensity. It was originally felt that maintaining all the spins to be decoupled in a saturated state would be sufficient, provided at some time they were periodically driven hard enough for full decoupling to occur. This was supported by a scheme for high-efficiency decoupling by Levy, Peat, Rosanske, and Parks.[8] Full nuclear Overhauser effects were retained in FT spectra if the decoupler power was reduced to saturation level during pulse delay and gated to full power during acquisition. The results of all the tests of wide band swept centerband modulated decoupling show that decoupling is quantized only at the time of acquisition. This is in agreement with the theoretical residual splittings from Equation (11).

1. The Wide Band Case

A saturated solution of p-chloronitrobenzene in ethyl acetate has a range of proton resonances that cover approximately 8 ppm as shown in Fig. 13. This sample therefore makes a good reference for determining wide band decoupling effectiveness. By using an offset of 16,800 Hz from 60,000,000 Hz as a center frequency, spectra were collected with swept centerband decoupling. An offset of 16,500 Hz was previously determined to be the proton resonance of TMS with a deuteriochloroform lock.

A ^{1}H scan width of 750 Hz (12.5 ppm) was used to prevent band-edge effects, and the scan rate of the decoupler was varied from 7.5 Hz to 75 Hz. If the scan rate exceeds approximately one tenth the scan width, the approximation of a rectangular power spectrum begins to fail due to secondary modulation. If the scan rate exceeds the scan width, the power spectrum will produce large harmonic sidebands outside of the scan width, and will begin to resemble swept square wave decoupling. The effect of varying the scan rate may be seen in Fig. 14. As the scan rate is increased, it causes a larger uncertainty in the single frequency bandwidth which, when averaged over the proton spectrum, gives a smaller residual splitting. As the scan rate continues to increase, the secondary modulation effects begin to dominate and the power spectrum density decreases rapidly. The transition to secondary modulation effects occurs at approximately 1/15 the scan width; for a 750Hz width the transition occurs at a scan rate of about 40 Hz.

A comparison of single frequency, noise, and swept centerband modulation decoupling is found in Fig. 15 Power levels were equivalent in all three cases and the swept centerband spectrum was taken under optimal conditions. The effect of swept centerband modulation can be seen to be that of averaging a single frequency response over the bandwidth swept.

2. The Narrow Band Case

Selective decoupling experiments monitor the change in residual coupling as a function of center frequency offset. From a plot of residual splitting vs. the offset, heteronuclear couplings can be determined.

The resolution for selective decoupling is limited by the rate at which the residual splitting changes per unit of offset. The best rate of change is found to be for single frequency decoupling (Eqn. (2)). However, it is often not very convenient to use the small increments in offset required for this method. A test of swept centerband modulation for selective decoupling is demonstrated in Fig. 16. A scan width of 100 Hz and scan rate of 15 Hz were used, and the offset was varied to determine the effectiveness of this approach. The intensity (related to $1 / b_r$) of the ^{13}C peak of dioxane falls quite rapidly with changes in offset but is nearly flat over the offsets where the Larmor frequency falls within the scan width. The slope corresponds to the theoretical dependence of residual splitting for a single frequency.

A comparison of selective decoupling using noise and swept centerband modulation methods was performed using the p-chloro-nitrobenzene in ethyl acetate sample. Proton modulation widths of 60 Hz (1 ppm) were used and the offset stepped by 60 Hz to cover a 540 Hz range (9 ppm). Fig. 17 shows the response of noise modulated decoupling with a 33.3 ms clock setting on the noise generator placed in INFINITE cycle RUN mode. Fig. 18 demonstrates the response of swept centerband modulation with a 60-Hz scan width and a scan rate of 10 Hz. Comparison shows that peak intensities are nearly the same for Larmor frequencies within the modulation width, but the rate of change of residual coupling is larger for swept centerband modulation than for noise modulation.

IV. Conclusion

Swept centerband modulated decoupling behaves as a single coherent frequency time averaged over the desired scan width, provided the scan rate remains much smaller than the scan width. Averaging over wide scan widths produces residual splittings much larger than is desired for good wide band response in FT spectra. In circumstances where absolute minimum residual splitting is not required, swept centerband modulation can provide uniform response over a desired scan width. Future applications of this technique are expected to be found in selective decoupling experiments.

An extension of the results from swept centerband decoupling experiments may be applied to swept square wave decoupling. Since sweeping any modulation will produce an averaging of the residual splitting response, swept square wave modulation will produce a response equal to an average of best and worst cases for coherent square wave modulation. For FT spectra collected using 50% swept square wave modulation the residual splitting can never be zero.

Future work in the area of wide band decoupling will be concentrated around the elimination of power outside the desired bandwidth. Two possible schemes are indicated, but both require modifications of the decoupling channel on a major scale. The first is synthesized modulation from the inverse FT of the proton spectra to be decoupled. The second is pulse decoupling, which requires a high power proton pulse amplifier. Both schemes have great potential for lowering the average power dissipated at the probe without losing decoupler effectiveness.

REFERENCES

1. W. A. Anderson and F. A. Nelson, J. Chem. Phys. 39, 183 (1963)
2. R. Freeman and W. A. Anderson, J. Chem. Phys. 42, 1199 (1965)
3. R. R. Ernst, J. Chem. Phys. 45, 3845 (1966)
4. G. C. Levy and G. L. Nelson, "Carbon-13 Nuclear Magnetic Resonance for Organic Chemists", Wiley-Interscience (New York)1972
5. A. Allerhand, R. F. Childers and E. Oldfield, J. Magn. Resonance, 11, 273 (1973)
6. Experience with Caltech's WH-180 30mm probe.
7. J. B. Grutzner and R. E. Santini, J. Magn. Resonance, 19, 173(1975)
8. G. C. Levy, I. R. Peat, R. Rosanske and S. Parks, J. Magn. Resonance, 18, 205(1975)

Appendix A

$$2\pi J_r = \left[(\Delta\omega - \pi J)^2 + (\gamma^S H_2)^2\right]^{\frac{1}{2}} - \left[(\Delta\omega + \pi J)^2 + (\gamma^S H_2)^2\right]^{\frac{1}{2}}$$

where $\Delta\omega = \omega_S - \omega_2$

For swept centerband, ω_2 goes linearly from $\omega_0 - \omega_{d/2}$ to $\omega_0 + \omega_{d/2}$. Let $\Delta\omega = \xi$, $d\xi = d(\omega_S - \omega_2) = -d\omega_2$ then the normalization factor for ω_2 becomes:

$$-\int_{\omega_0-\omega_{d/2}}^{\omega_0+\omega_{d/2}} d\xi = -\xi\Big|_{\omega_0-\omega_{d/2}}^{\omega_0+\omega_{d/2}} = -\omega_d$$

Therefore:

$$J_{r(\text{average})} = \frac{1}{2\pi\omega_d}\int_{\omega_0-\omega_{d/2}}^{\omega_0+\omega_{d/2}} \left[(\xi - \pi J)^2 + (\gamma^S H_2)^2\right]^{\frac{1}{2}} - \left[(\xi + \pi J)^2 + (\gamma^S H_2)^2\right]^{\frac{1}{2}} d\xi$$

Let $E = \pi J$

$F = \gamma^S H_2$

Then $J_{r(\text{ave})} = \frac{1}{2\pi\omega_d}(I_1 - I_2)$

where $I_1 = \int_{\omega_0-\omega_{d/2}}^{\omega_0+\omega_{d/2}} \left[(\xi - E)^2 + F^2\right]^{\frac{1}{2}} d\xi$

$I_2 = \int_{\omega_0-\omega_{d/2}}^{\omega_0+\omega_{d/2}} \left[(\xi + E)^2 + F^2\right]^{\frac{1}{2}} d\xi$

of the form

$$\int (ax^2 + bx + c)^{\frac{1}{2}}\, dx$$

$$= \frac{2cx+b}{4c}\,(ax^2 + bx + c)^{\frac{1}{2}} + \frac{4ac - b^2}{8c} \int (ax^2 + bx + c)^{-\frac{1}{2}}\, dx \qquad \text{(note 1)}$$

$$\int (ax^2 + bx + c)^{-\frac{1}{2}}\, dx = (c)^{-\frac{1}{2}} \operatorname{arcsinh}\left[(2cx+b)(4ac - b^2)^{-\frac{1}{2}}\right] \qquad \text{(note 2)}$$

For I_1 $\quad a = E^2 + F^2$

$\quad b = -2E$

$\quad c = 1$

For I_2 $\quad a = E^2 + F^2$

$\quad b = 2E$

$\quad c = 1$

$$I_1 = \frac{2\xi - 2E}{4}\left((\xi - E)^2 + F^2\right)^{\frac{1}{2}} + \frac{4(E^2+F^2) - 4E^2}{8} \operatorname{arcsinh}\left[\frac{2\xi - 2E}{4}\,(4(E^2+F^2) - 4E^2)^{-\frac{1}{2}}\right]$$

$$= \frac{\xi - E}{2}\left((\xi - E)^2 + F^2\right)^{\frac{1}{2}} + \frac{F^2}{2} \operatorname{arcsinh}\left(\frac{\xi - E}{F}\right)$$

$$I_2 = \frac{2\xi + 2E}{4}\left((\xi + E)^2 + F^2\right)^{\frac{1}{2}} + \frac{4(E^2+F^2) - 4E^2}{8} \operatorname{arcsinh}\left[\frac{2\xi + 2E}{4}\,(4(E^2+F^2) - 4E^2)^{-\frac{1}{2}}\right]$$

$$= \frac{\xi + E}{2}\left((\xi + E)^2 + F^2\right)^{\frac{1}{2}} + \frac{F^2}{2} \operatorname{arcsinh}\left(\frac{\xi + E}{F}\right)$$

Note 1: CRC Standard Mathematical Tables, 16th Edition, Table of Integrals, No. 242, pg. 424.

Note 2: CRC Standard Mathematical Tables, 16th Edition, Table of Integrals, No. 237, pg. 423.

Therefore,

$$J_{r(ave)} = \frac{1}{4\pi\omega_d}\left[(\Delta\omega - \pi J)\left[(\Delta\omega - \pi J)^2 + (\gamma^S H_2)^2\right]^{\frac{1}{2}} + (\gamma^S H_2)^2 \operatorname{arcsinh}\left(\frac{\Delta\omega - \pi J}{\gamma^S H_2}\right) - (\Delta\omega + \pi J)\left[(\Delta\omega + \pi J)^2 + (\gamma^S H_2)^2\right]^{\frac{1}{2}} - (\gamma^S H_2)^2 \operatorname{arcsinh}\left(\frac{\Delta\omega + \pi J}{\gamma^S H_2}\right)\right] \Bigg|_{\omega_S - (\omega_o - \omega_d/2)}^{\omega_S - (\omega_o + \omega_d/2)}$$

Appendix B

Calculation of decoupling field

Coil: 2 turns 1.78 cm × 1.78 cm × 1.78 cm

matched to 50 ohms impedance

VSWR ≃ 1 → purely resistive load

Maximum power out of ENI 350L

(0 dB attenuation) 20 W

filter attenuation 2.3 dB

Maximum power at coils 11.8 W

$$I_{rms} = \sqrt{\frac{P_{rms}}{R}} = \sqrt{\frac{11.8}{50}} = 0.485 \text{ Amp}$$

$$H_2 = \mu_0 i n$$

$$= \left(4\pi \times 10^{-7} \frac{\text{Weber}}{\text{Amp - Meter}}\right) \left(0.485 \text{ Amp}\right) \left(\frac{1 \text{ turn}}{8.9 \times 10^3 \text{ Meter}}\right)$$

$$\times 10^4 \text{ gauss per } \frac{\text{Weber}}{\text{Meter}^2}$$

$$= 0.685 \text{ gauss}$$

γ^S for proton is $2.79 \times 10^4 \frac{\text{radian}}{\text{sec}} (\text{gauss})^{-1}$

$$\frac{H_2 \gamma^S}{2\pi} = (0.685 \text{ gauss}) (2.79 \times 10^4 \frac{\text{rad}}{\text{sec}} (\text{gauss})^{-1})/2\pi \text{ (rad)}$$

$$= 3040 \text{ Hz}$$

$$\frac{P_{out}}{P_{in}} = 10^{\frac{dB}{10}} \text{ (attenuation)}$$

$$H_2 = 3040 H_S (10^{A/10})^{\frac{1}{2}}$$

where A is the attenuation in dB.

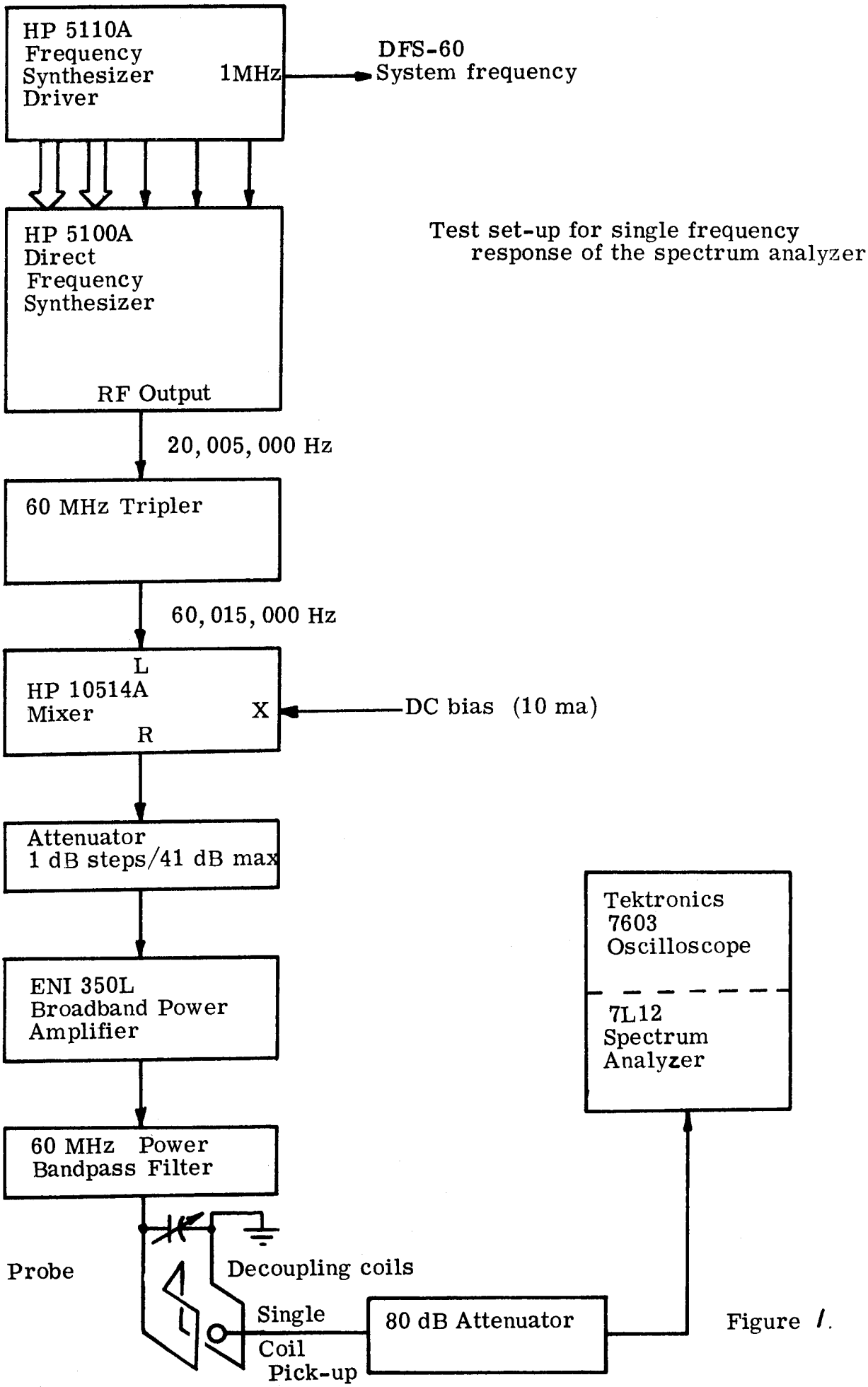

Test set-up for single frequency response of the spectrum analyzer

Figure 1.

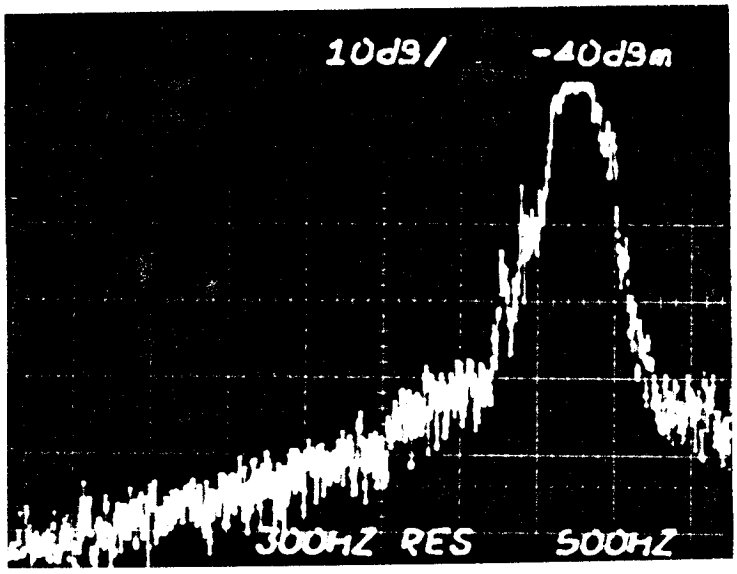

60, 015, 000 Hz

Figure 2 Single frequency response power spectrum

Vertical 10 dB/Div
Horizontal 500 Hz/Div

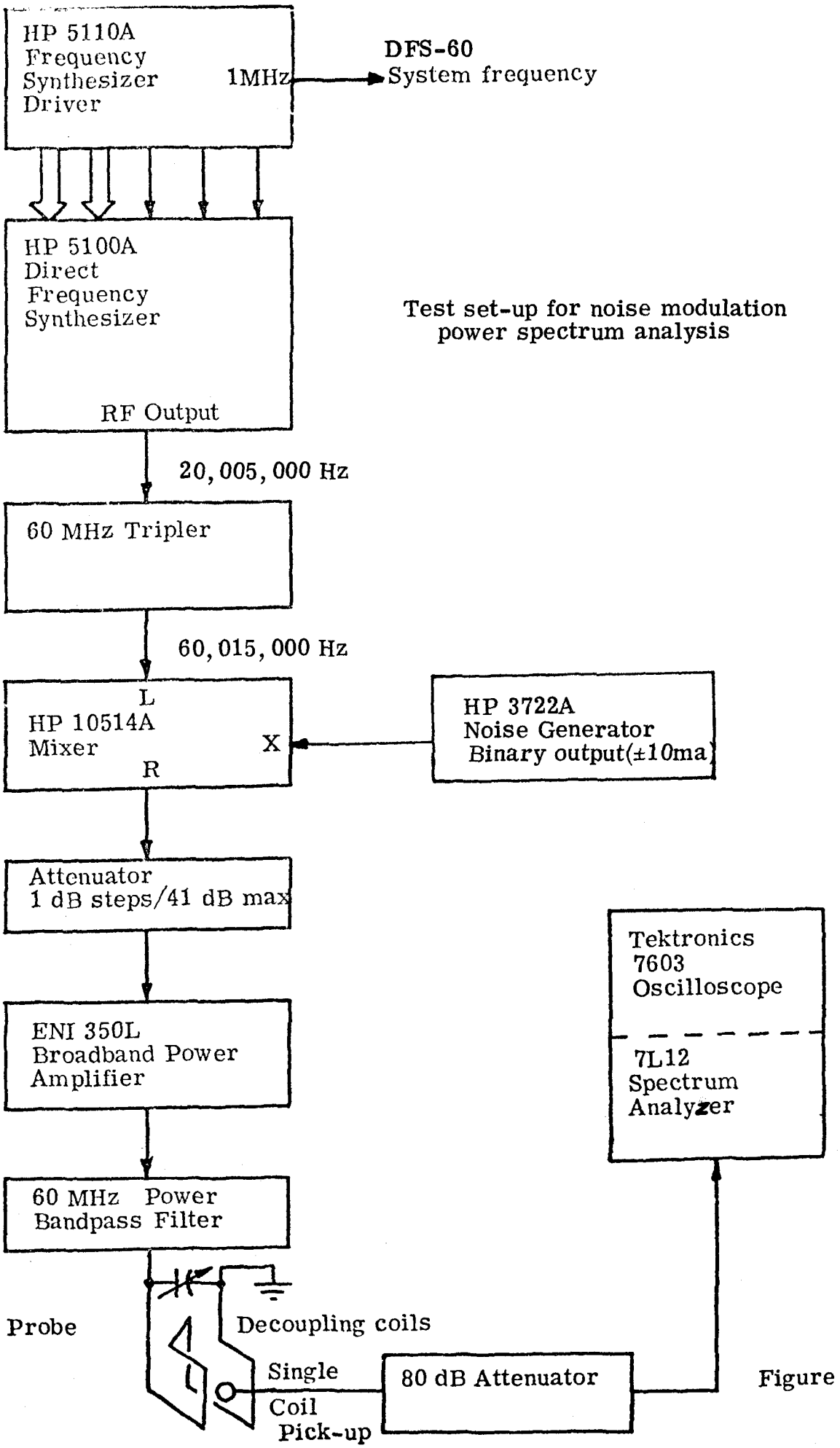

Test set-up for noise modulation power spectrum analysis

Figure 3

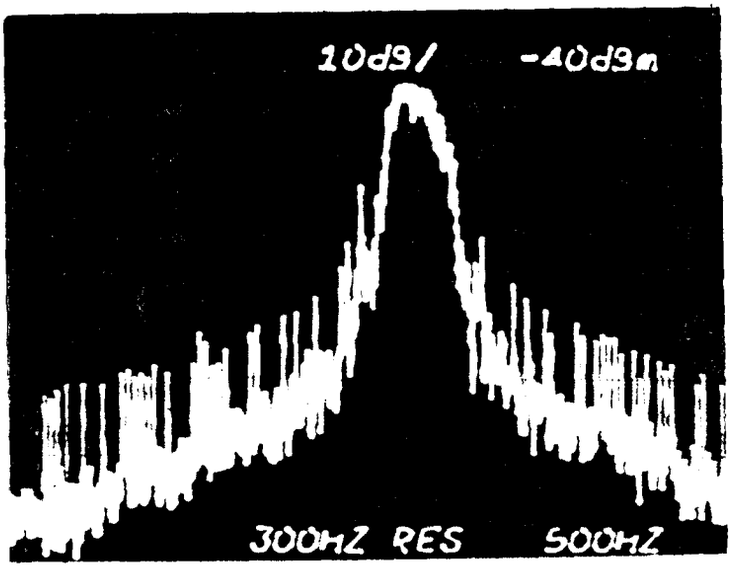

60,015,000 Hz

Figure 4a Noise modulation power spectrum

Clock period	33.3 msec	Vertical	10 dB/Div
Cycle length	INFINITE	Horizontal	500 Hz/Div

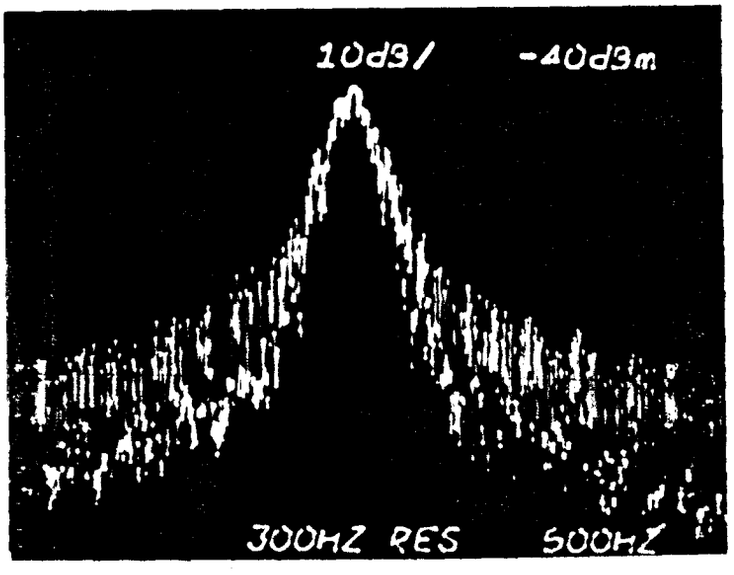

60,015,000 Hz

Figure 4b Noise modulation power spectrum

Clock period	10 msec	Vertical	10 dB/Div
Cycle length	INFINITE	Horizontal	500 Hz/Div

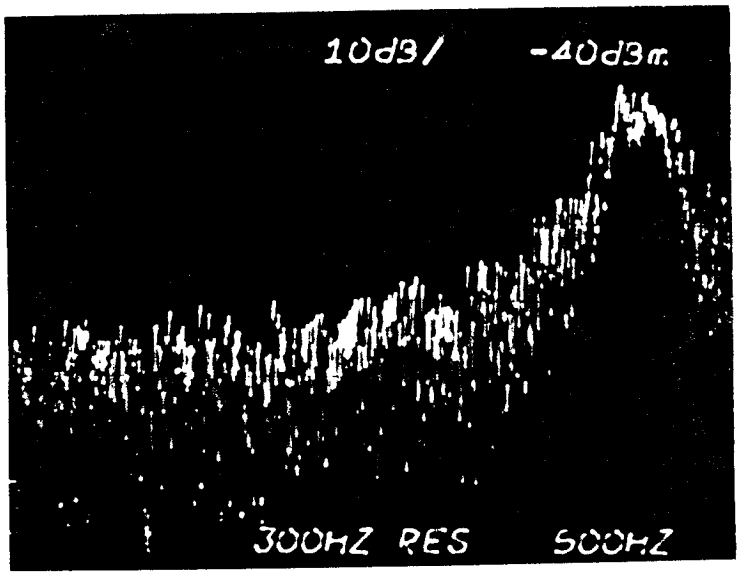

60, 015, 000 Hz

Figure 4c Noise modulation power spectrum

Clock period	3.33 msec	Vertical	10 dB/Div
Cycle length	INFINITE	Horizontal	500 Hz/Div

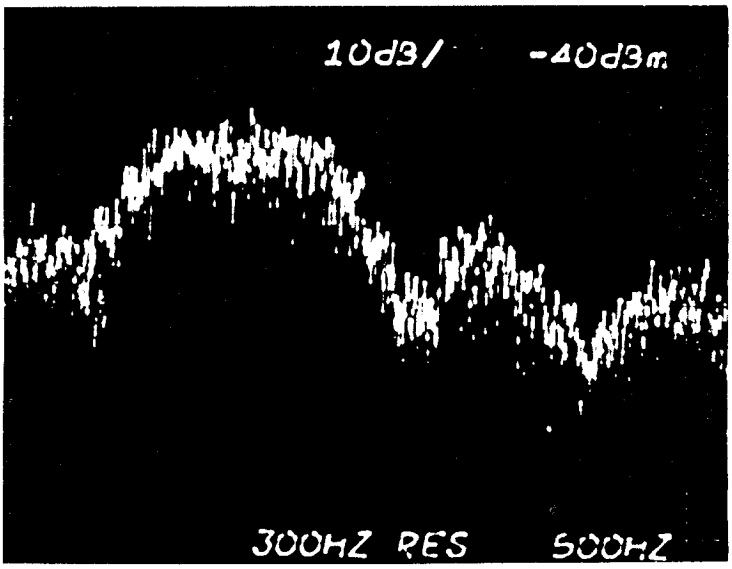

60, 015, 000 Hz

Figure 4d Noise modulation power spectrum

Clock period	1 msec	Vertical	10 dB/Div
Cycle length	INFINITE	Horizontal	500 Hz/Div

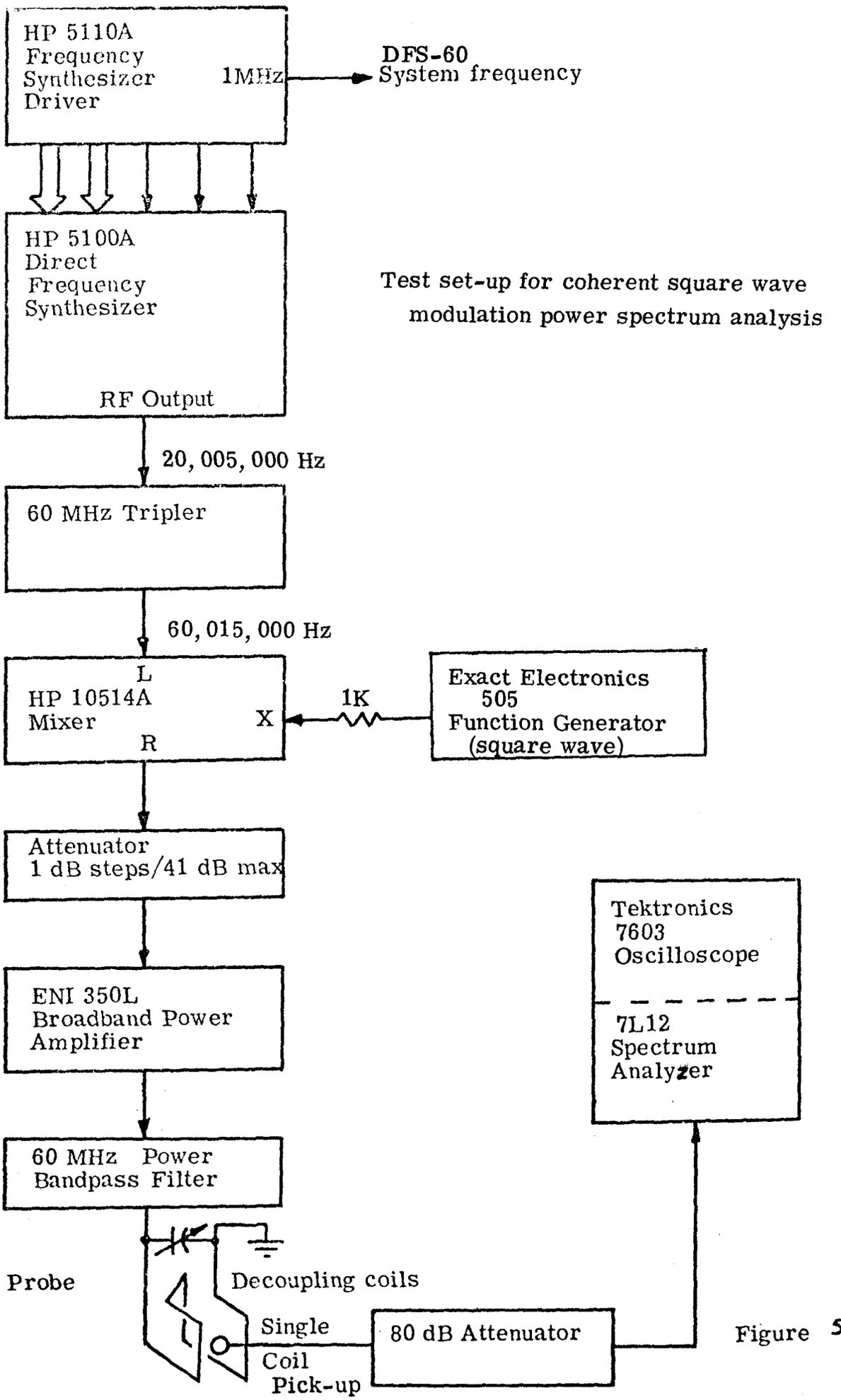

Test set-up for coherent square wave modulation power spectrum analysis

Figure 5

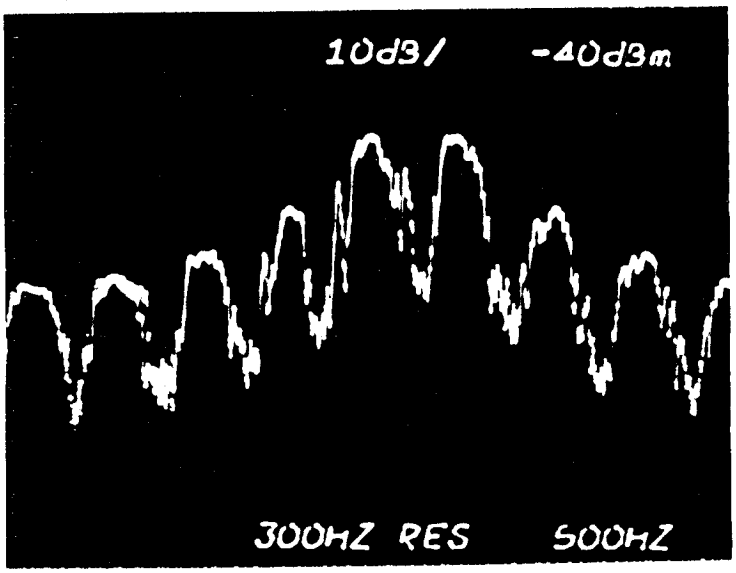

60, 015, 000 Hz

Figure 6a Square wave modulation power spectrum
Modulation frequency 300 Hz Vertical 10 dB/Div
Horizontal 500 Hz/Div

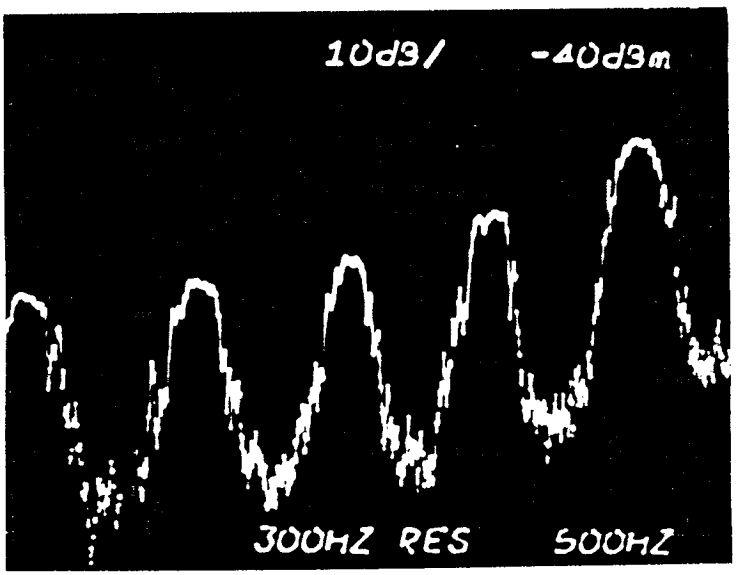

60, 015, 000 Hz

Figure 6b Square wave modulation power spectrum
Modulation frequency 500 Hz Vertical 10 dB/Div
Horizontal 500 Hz/Div

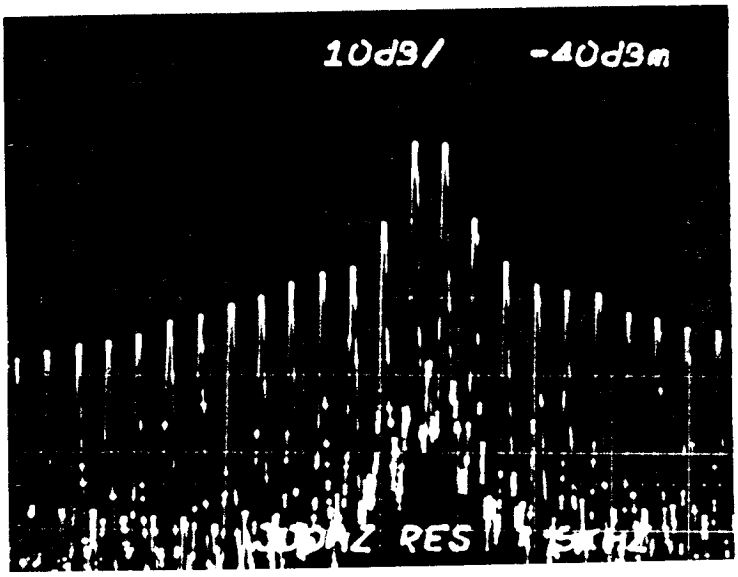

60, 015, 000 Hz

Figure 6c Square wave modulation power spectrum

Modulation frequency	1000 Hz	Vertical	10 dB/Div
		Horizontal	5000 Hz/Div

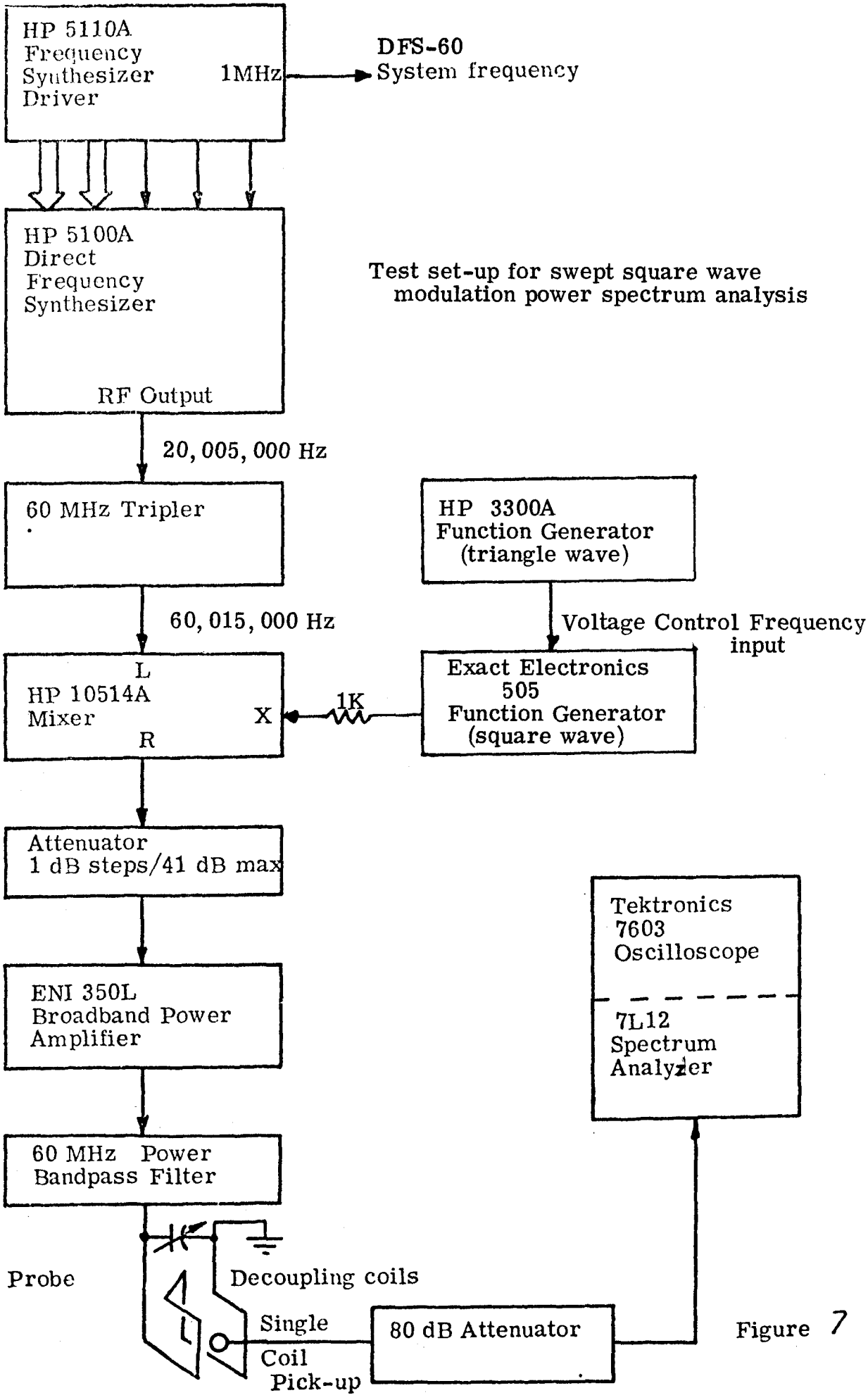

Test set-up for swept square wave modulation power spectrum analysis

Figure 7

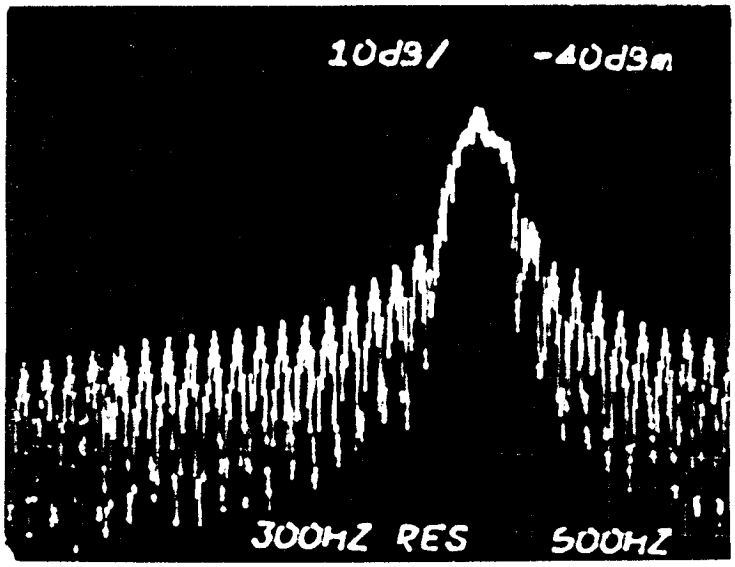

60, 015, 000 Hz

Figure 8a Swept square wave modulation power spectrum

Modulation range 50 Hz - 200 Hz Vertical 10 dB/Div

Modulation frequency 10 Hz Horizontal 500 Hz/Div

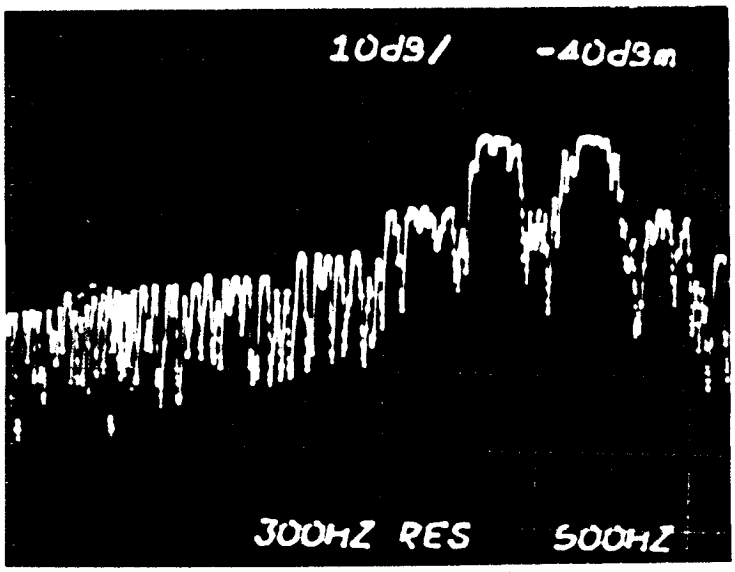

60, 015, 000 Hz

Figure 8b Swept square wave modulation power spectrum

Modulation range 400 Hz - 650 Hz Vertical 10 dB/Div

Modulation frequency 10 Hz Horizontal 500 Hz/Div

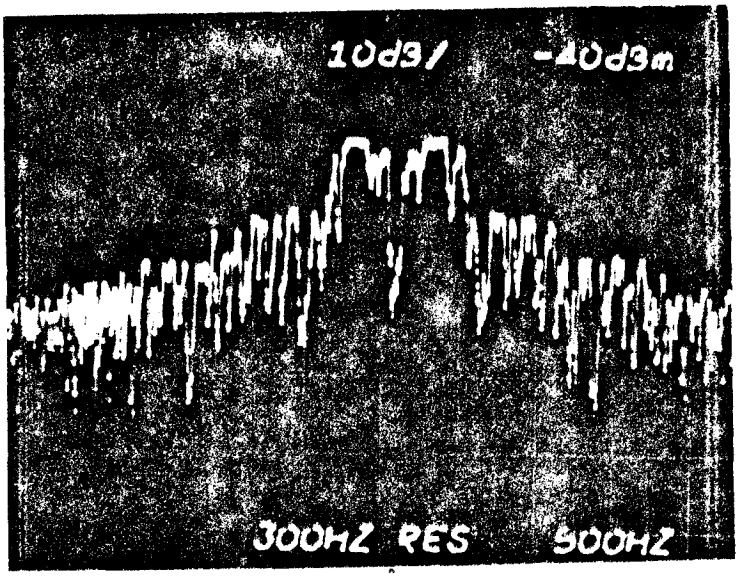

60, 015, 000 Hz

Figure 8c Swept square wave modulation power spectrum

Modulation range 300 Hz - 750 Hz
Modulation frequency 10 Hz
Vertical 10 dB/Div
Horizontal 500 Hz/Div

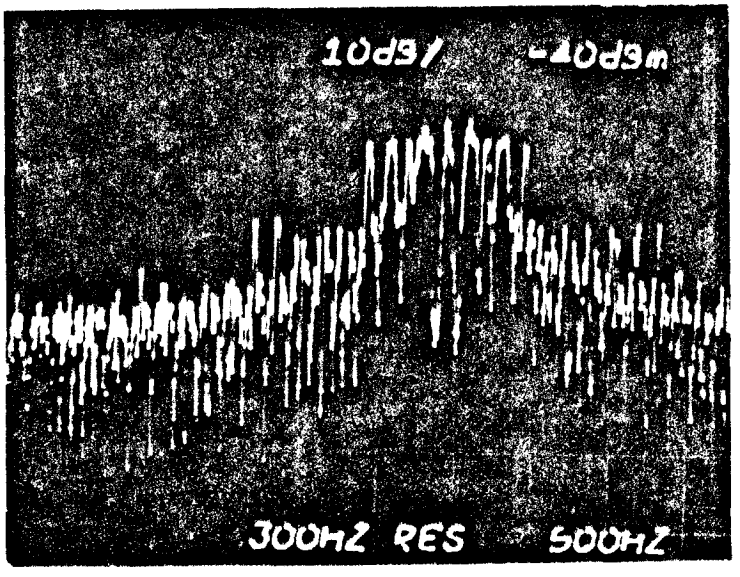

60, 015, 000 Hz

Figure 8d Swept square wave modulation power spectrum

Modulation range 250 Hz - 1000 Hz
Modulation frequency 10 Hz
Vertical 10 dB/Div
Horizontal 500 Hz/Div

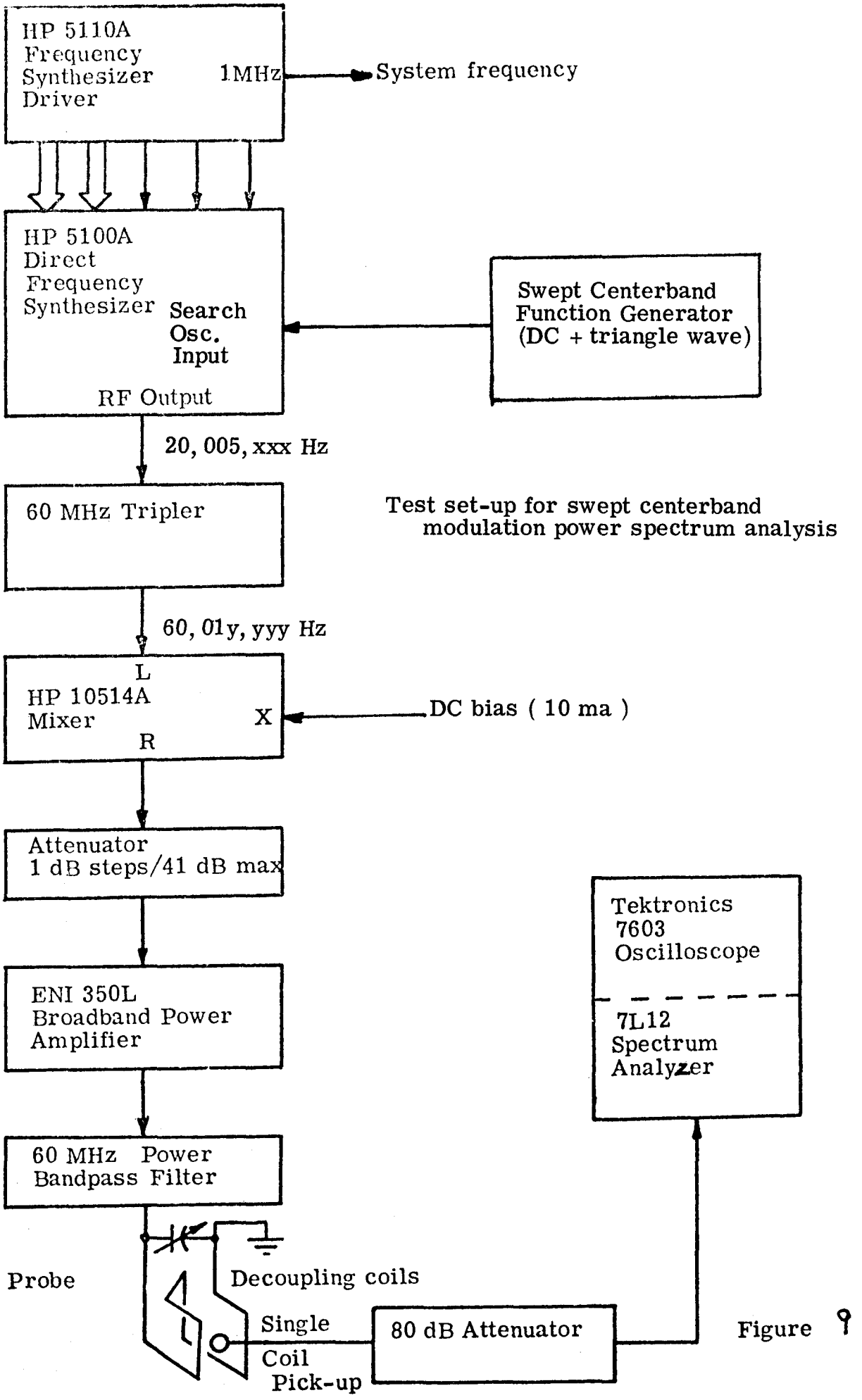

Test set-up for swept centerband modulation power spectrum analysis

Figure 9

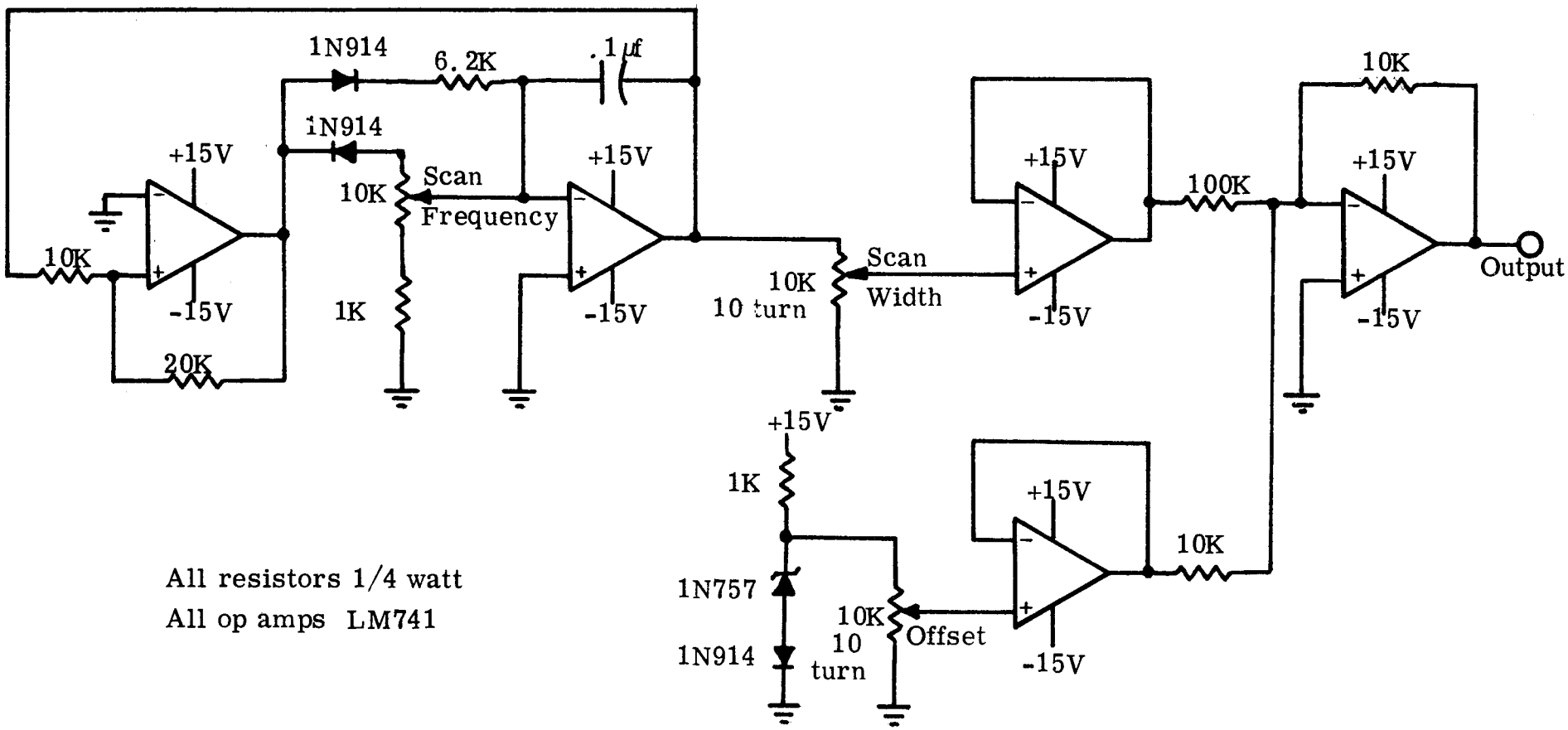

Figure 10 Schematic for swept centerband driver

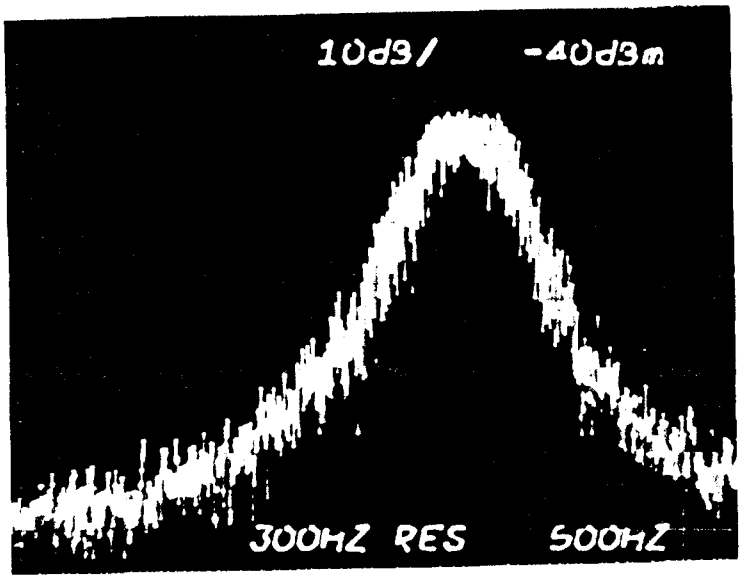

60, 015, 000 Hz

Figure 11a Swept centerband power spectrum.

Scan width	500 Hz	Vertical	10 dB/Div
Scan repetition	75 Hz	Horizontal	500 Hz/Div

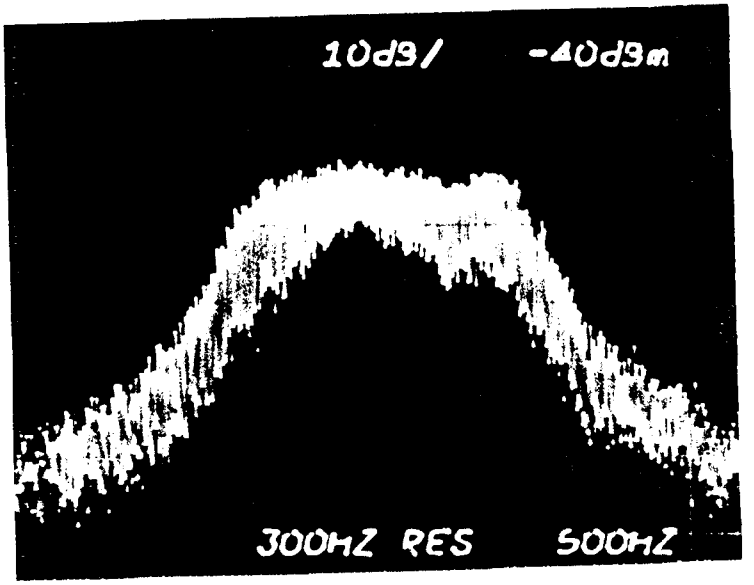

60, 015, 000 Hz

Figure 11b Swept centerband power spectrum

Scan width	1500 Hz	Vertical	10 dB/Div
Scan repetition	75 Hz	Horizontal	500 Hz/Div

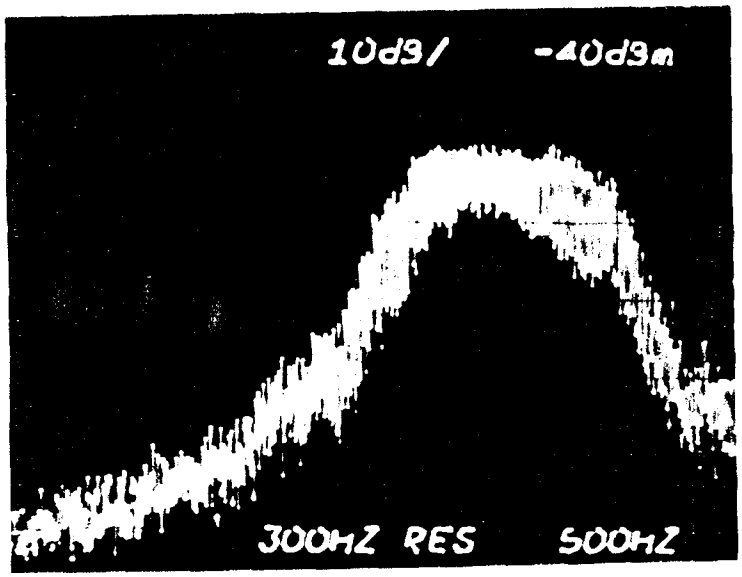

60, 015, 000 Hz

Figure 11c Swept centerband power spectrum

Scan width	1000 Hz	Vertical	10 dB/Div
Scan repetition	75 Hz	Horizontal	500 Hz/Div

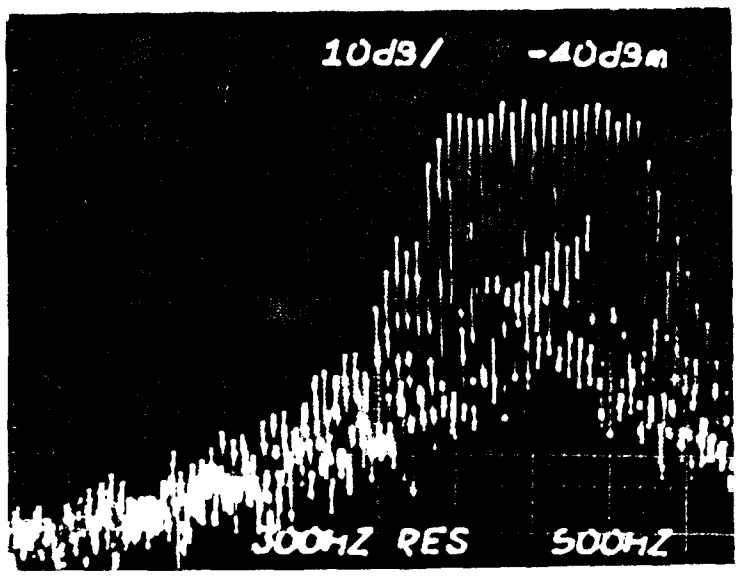

60, 015, 000 Hz

Figure 11d Swept centerband power spectrum

Scan width	1000 Hz	Vertical	10 dB/Div
Scan repetition	20 Hz	Horizontal	500 Hz/Div

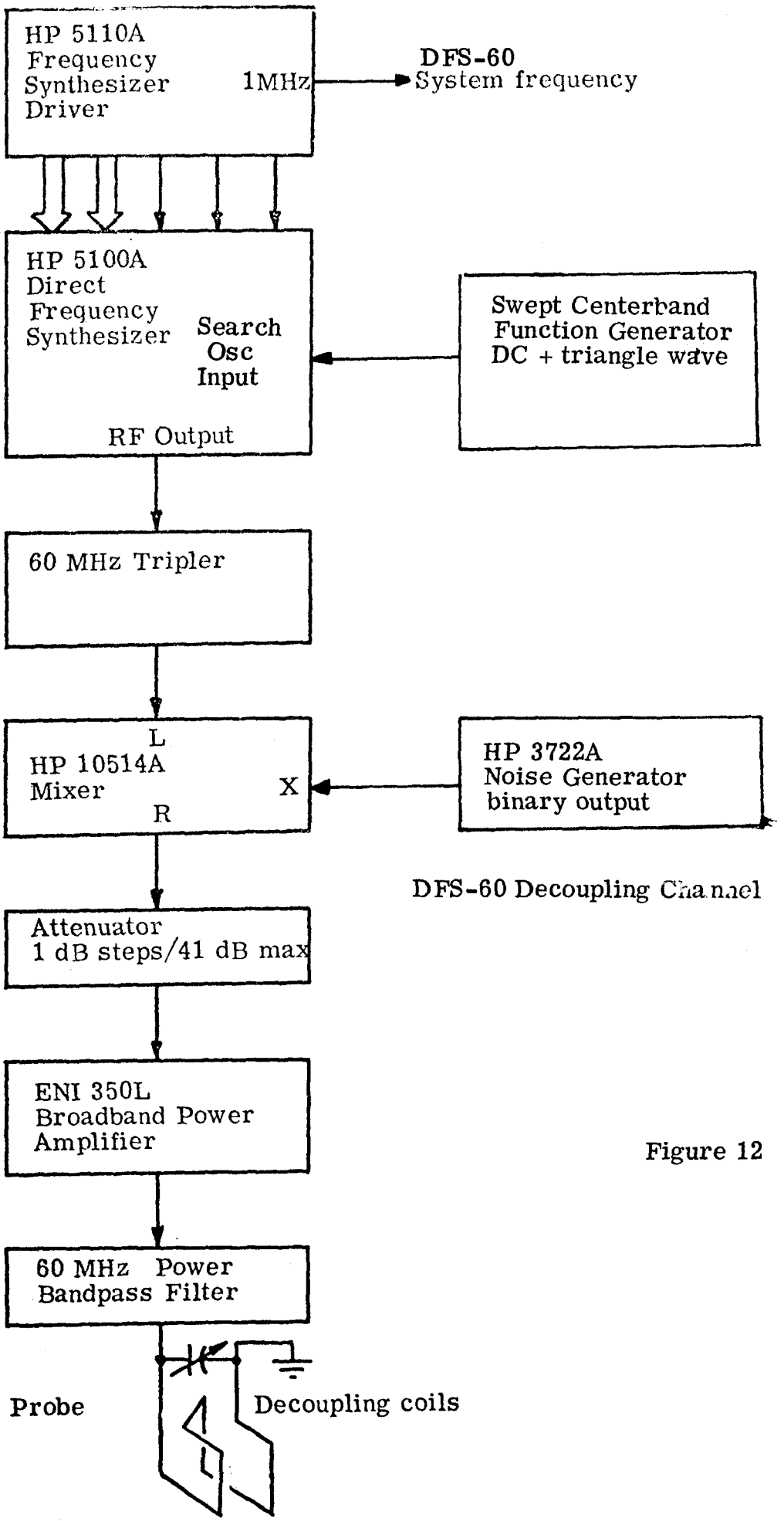

DFS-60 Decoupling Channel

Figure 12

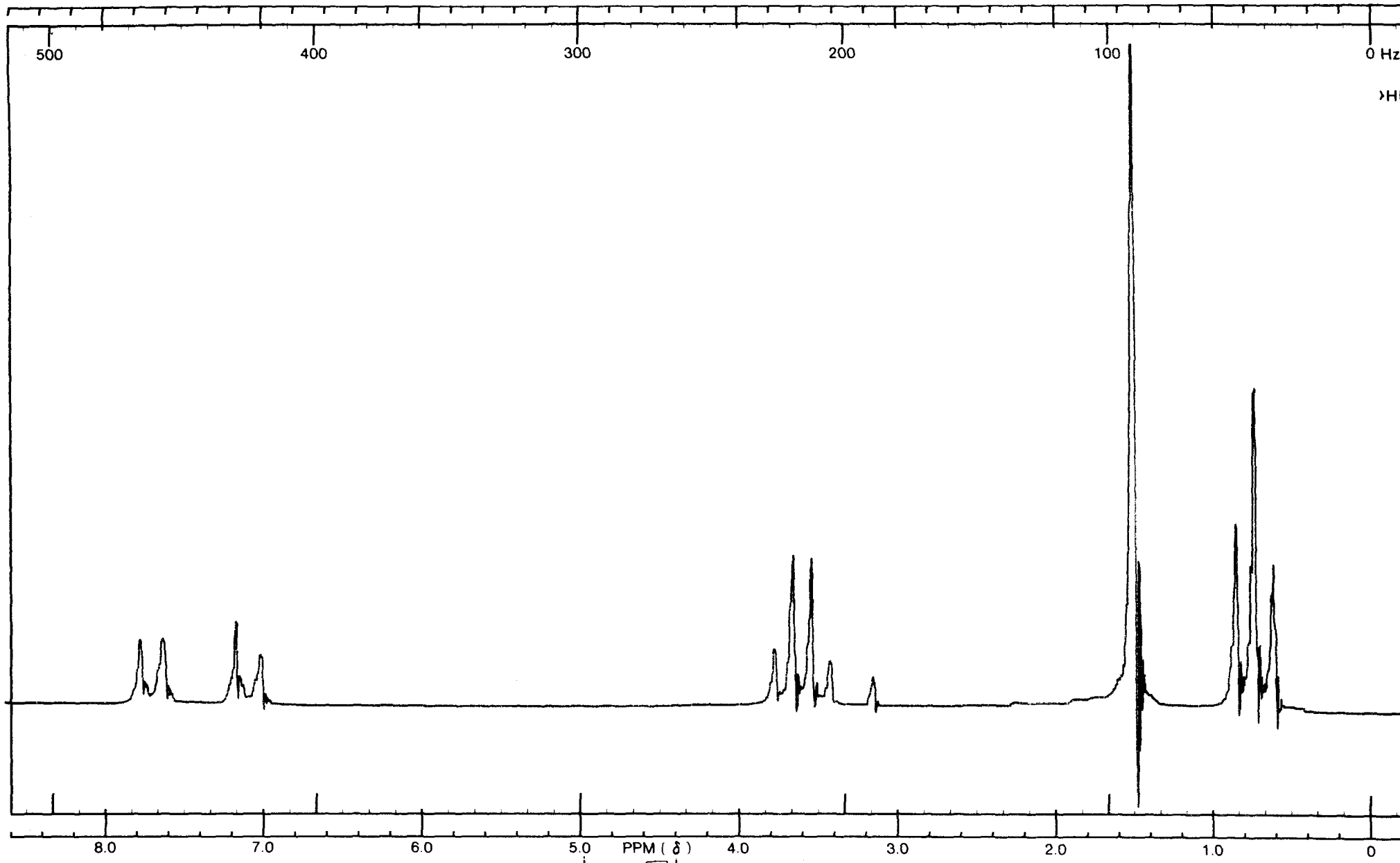

SWEEP OFFSET (Hz): 0
SPECTRUM AMPLITUDE: 1
INTEGRAL AMPLITUDE:
SPINNING RATE (RPS): 40

MANUAL
SWEEP TIME (SEC): 5 (250)
SWEEP WIDTH (Hz): 25 50 100 250 (500)
FILTER: (1) 2 3 4 5 6 7 8 (2)
RF POWER LEVEL: .05 (.05)

AUTO ☐

SAMPLE: sat. 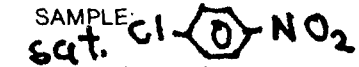 in E+Ac

SOLVENT:

REMARKS:

THOMPSON PACKARD (TPV 60T)
WILMAD (WCV 60T)

DATE:

OPERATOR

60 MHz NMR SPECTRUM NO. FIGURE 13

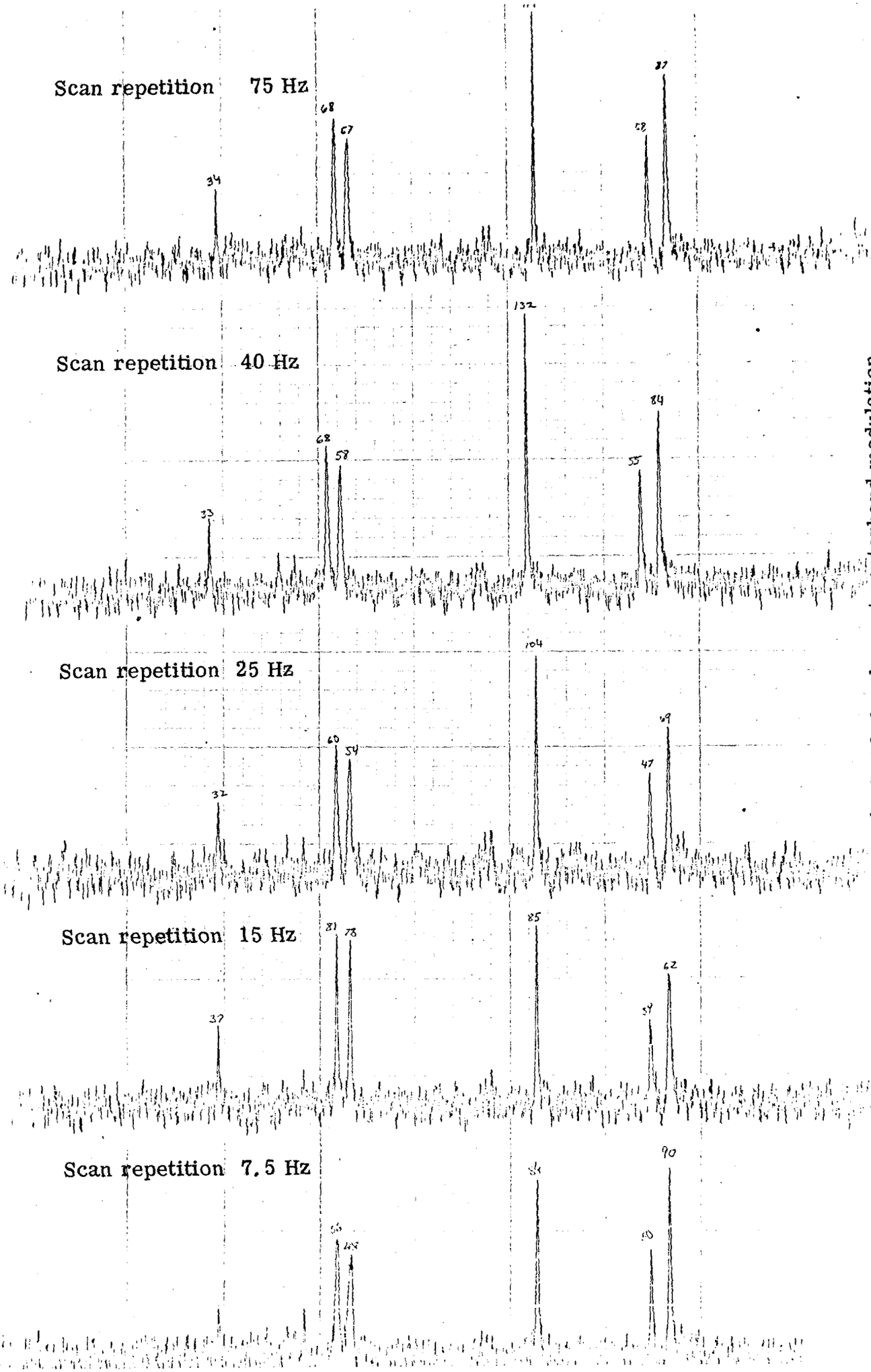

Figure 14 Decoupling response of wide band swept centerband modulation
Offset 16,600 Hz Scan width 750 Hz Power level at -3dB (see appendix B)

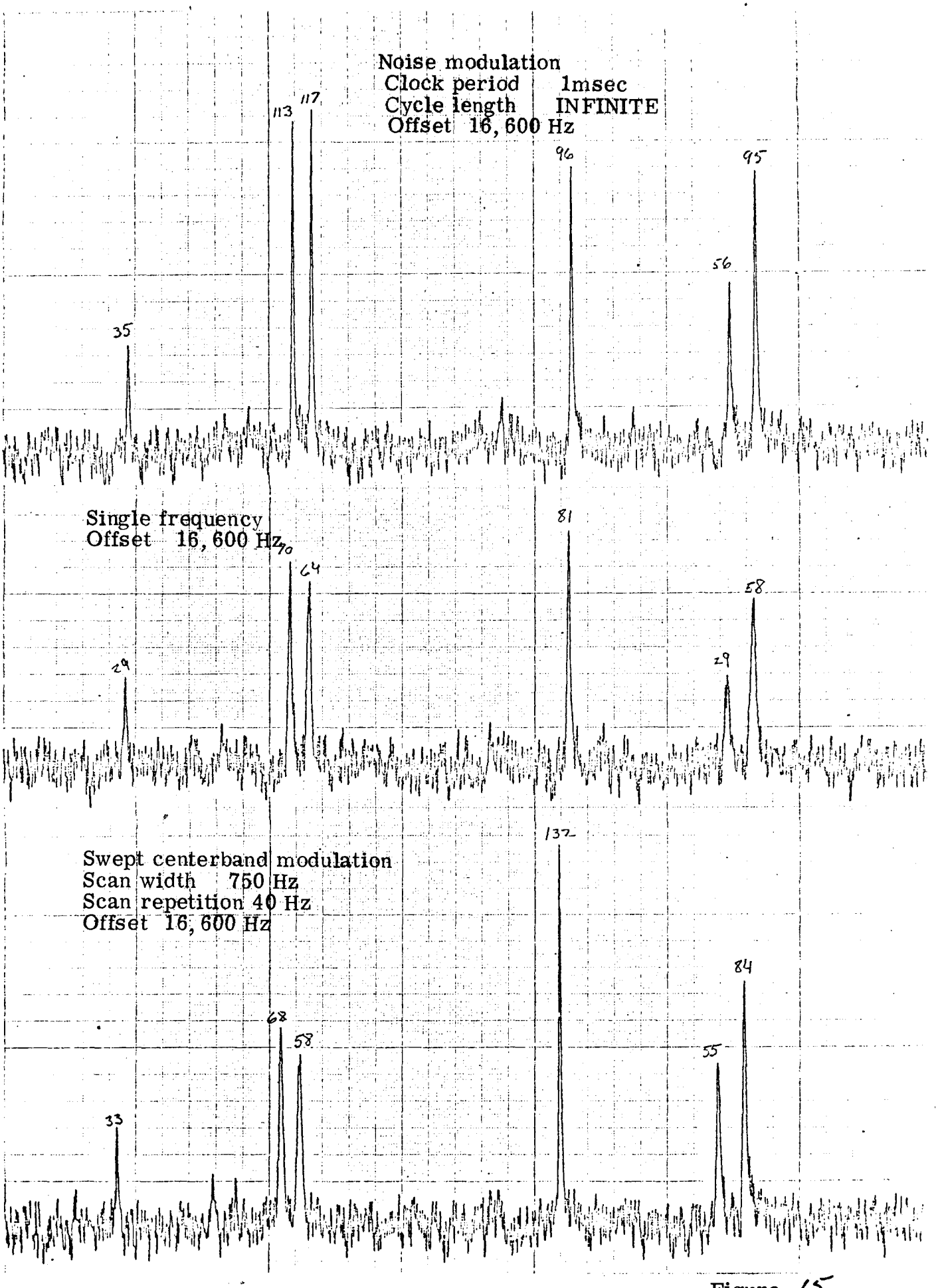

Figure 15

Wide band response - power level at -3dB(see appendix B)
Proton decoupled 13C spectra

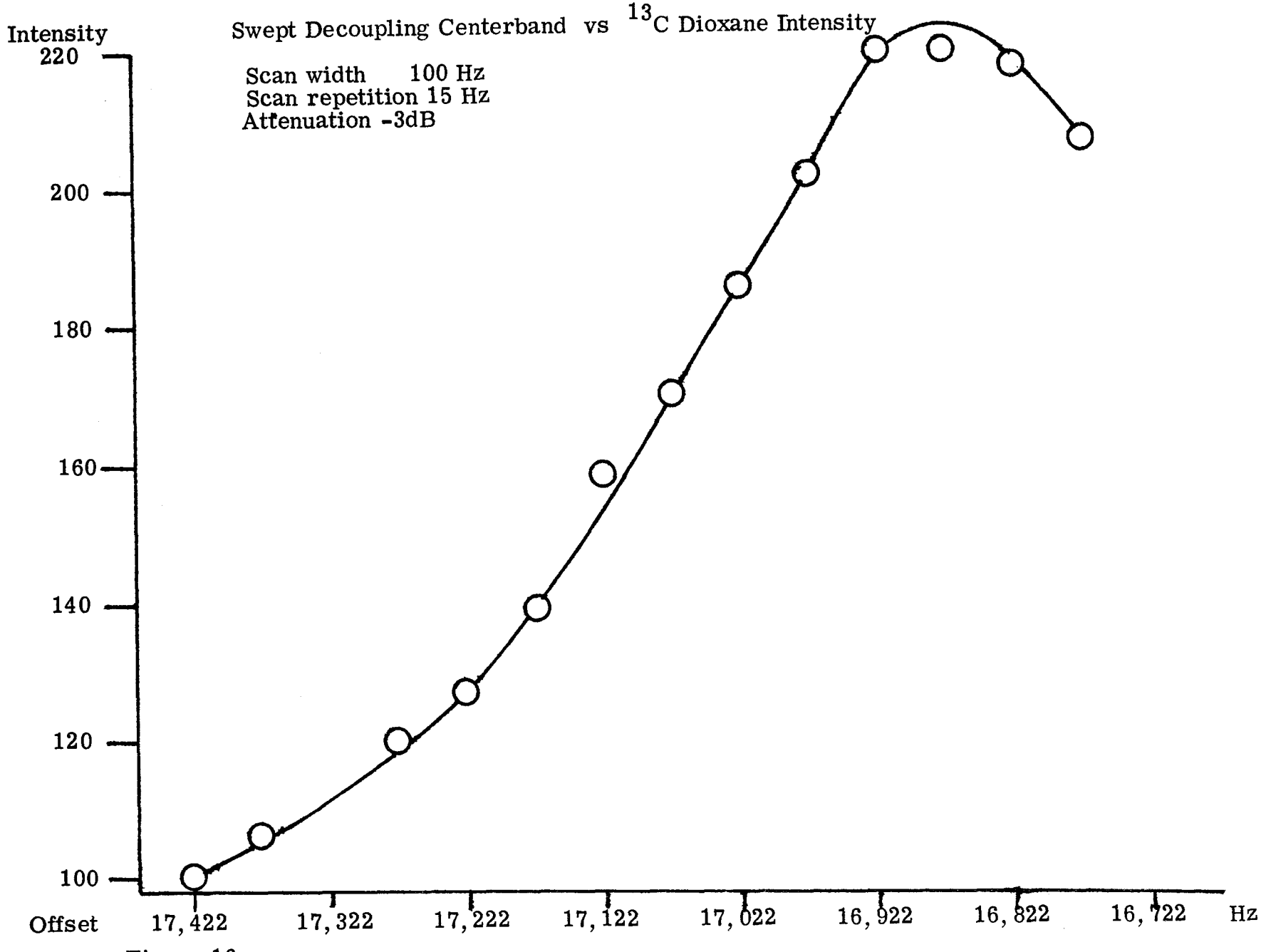
Swept Decoupling Centerband vs ^{13}C Dioxane Intensity
Scan width 100 Hz
Scan repetition 15 Hz
Attenuation -3dB
Intensity
220
200
180
160
140
120
100
Offset
17,422
17,322
17,222
17,122
17,022
16,922
16,822
16,722
Hz

Figure 16

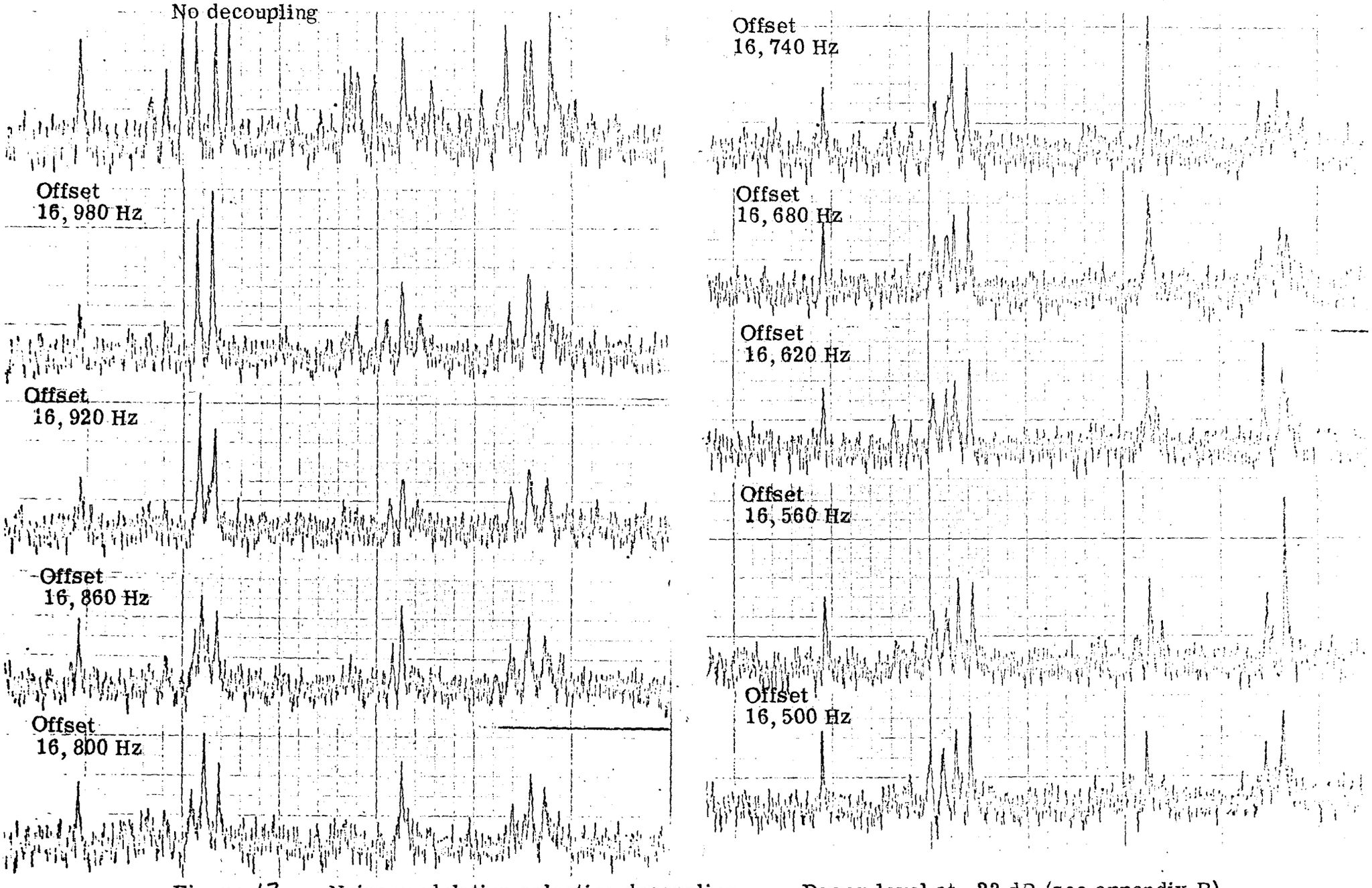

Figure 17 Noise modulation selective decoupling Power level at -23 dB (see appendix B)
Clock period 33.3msec Cycle length INFINITE Proton decoupled 13C spectra

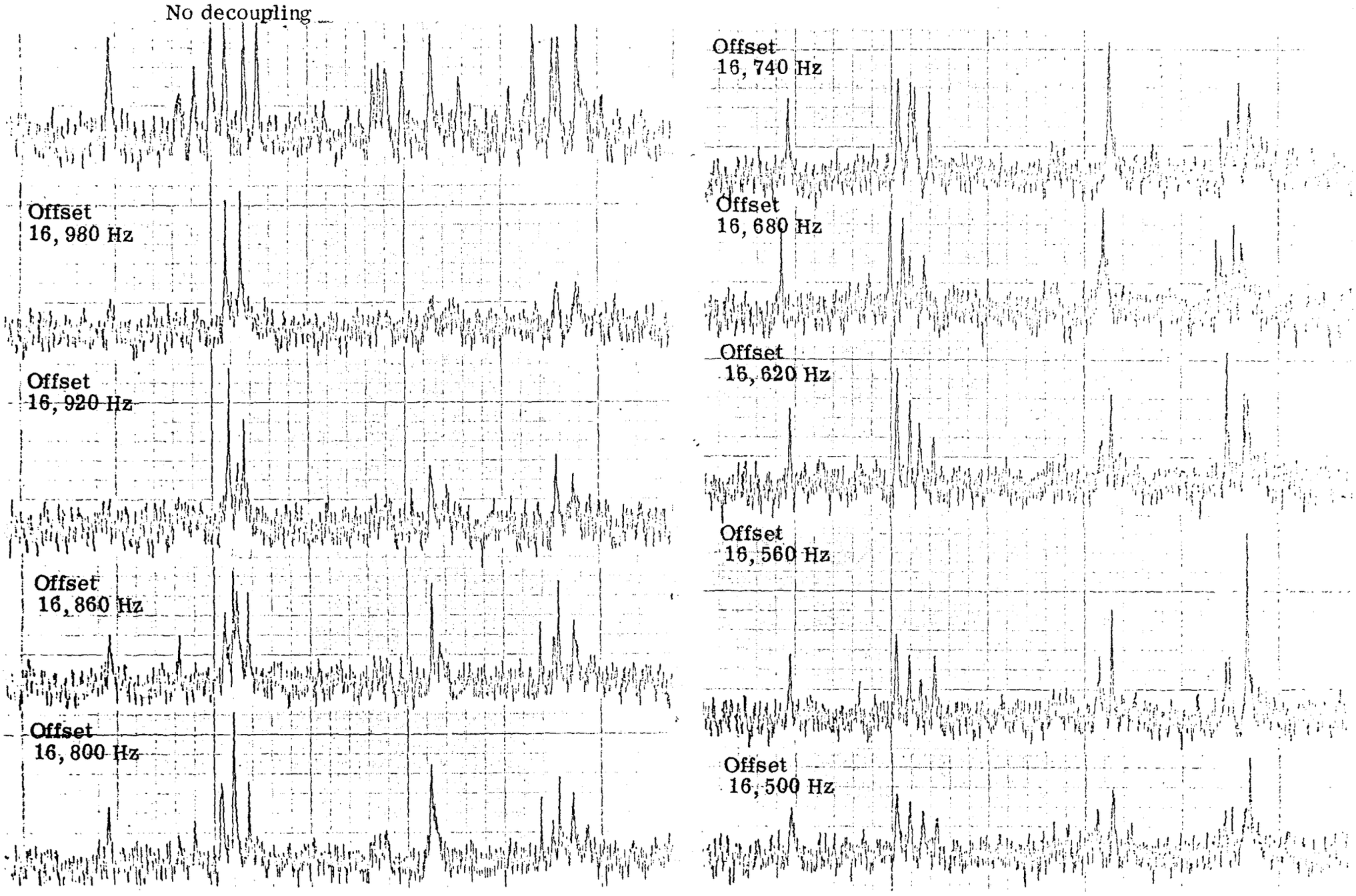

Figure 18 Swept centerband selective decoupling Power level at -23 dB(see appendix B)
Scan width 60 Hz Scan repetition 10 Hz Proton decoupled 13C spectra